

Iterative mathematical models based on curves and applications to coastal profiles

Fabio Caldarola, Manuela Carini, Mario Maiolo and Maria Anastasia Papaleo

Abstract. The object of study of this paper is iterative systems based on general types of curves, not only on circumference arcs. We begin by presenting some implementations and generalizations of constructions based on arcs of circumference. Then we consider constructions based on general curves and give a “universal property” relating to the primary construction that exploits arcs of circumference. With the prospect of applying these theoretical models also to coastal geomorphology in the future, and inspired by one of the best-known models on the subject, the logarithmic spiral one for the so-called headland-bay beaches (HBBs), we study geometrically some cases in which the constructions are based on arcs of the golden spiral. Simultaneously we concretely illustrate and explain the universal property above. Finally we dedicate a section to discuss the possibility of how to numerically evaluate and compare the (infinite) lengths originating from our theoretical geometric constructions. Some explicit examples, calculations and comparisons will be provided by the use of infinity computing which is one of the various possible assets that contemporary non-standard mathematics makes available.

Mathematics Subject Classification (2010). Primary 28A80; Secondary 11B39, 86A05, 03H05 .

Keywords. Iterative systems, recursive equations, fractals, Golden spiral, Fibonacci numbers, Coastal profiles, Headland-bay shaped beaches, infinity computing.

1. Introduction

The study of coastal profiles both from a geomorphological, physical-dynamic, or purely mathematical-geometric point of view has represented a formidable attraction for researchers from all over the world in the last century. In fact,

This work was completed with the support of our \TeX -pert.

the lenses adopted by researchers to investigate a system that is in itself highly complex and changeable from place to place were many and multiform. The existing literature includes thousands of works in the fields of mathematical physics, engineering, geology, etc., and have often inspired the birth of new research areas completely disconnected, but sometimes only apparently, from their origin.

This paper largely draws inspiration from one of the most widespread and ubiquitous coastal typologies around the globe, as well as one of the most studied and one of the first to receive attention: a *headland-bay beach* (usually abbreviated HBB) is the dynamic-evolutionary result which occurs in presence of a point of high land or a point of land or rock projecting into water. This interpretation could also be applied to ever smaller scales, given the differences in compactness, consistency, density, strength that naturally occur in various environments and contexts both at large and small and very small scales.

The best known models describing headland-bay beaches (HBBs) are the logarithmic spiral, hyperbolic tangent and parabolic models (see [21, 39, 55]). The small variants of these three fundamental models that have been proposed in the last fifty years are numerous (see [22] and its extensive bibliography) and, recently, a fourth different model of an elliptical type has also been presented (see [34]). But all the models and variants existing in the literature seem to be based on a single arc of a curve, i.e. spiral, hyperbola, parabola, ellipse, as mentioned above. Our starting idea however, to simplify as much as possible, is to consider not a single curve arc but several consecutive arcs, depending on the objectives and the level of precision that we want to achieve. In this point of view, the recursive model with arcs of circumference originally proposed in [23] fits well. We will first try to implement this system and generalize it for our purposes which go far beyond this paper. In fact, this work, rather than a point of arrival, should be understood as an initial push and start towards several research directions, some of which are strongly interconnected. To give more details, it is better to break down and describe the contents section by section.

In Sect. 2 we will build on the results of [23], enhancing and generalizing them to be used in wider contexts and, last but not least, also towards our goals, not only of this article. In particular, we will introduce a setting based on multi-indices which is indispensable for present and, above all, future developments. We will then transfer some simple but instructive “pilot” examples to the new setting (see Examples 2.1-2.5). Then we discuss the fractal dimension of the resulting set, i.e. the “end points set” $E(\mathcal{S})$, and we make some considerations on the previous explicit constructions. In particular, we also establish a result (see Proposition 2.1) which gives full details of an explicit and illuminating configuration which shows as the resulting set $E(\mathcal{S})$ of an arc-based system is not necessarily a fractal. Finally we will conclude the section by finding the corresponding polar equations (see (2.14)) of the arc-based recursive system (2.1).

In Sect. 3 we start the possibility of considering not only arcs of circumference on which to base a recursive system like (2.1), but quite general arcs of curves. In some cases, however, this turns out to be equivalent to a special system built with arcs of circumference: we have called this faculty a “universal property” of the arcs of circumference system (see Subsect. 3.1). Therefore, recalling the logarithmic spiral model originally proposed by [55] for headland-bay shaped beaches, we will examine in Subsect. 3.2 the golden spiral, in itself very important from both a theoretical and applied point of view, and in particular its arcs as fundamental building blocks for getting a recursive system based on curves other than the circumference. Examples 3.1 and 3.2 should be enlightening to the reader.

In Sect. 4 we will consider and start applications to coastal morphology. We will also talk about randomness in general recursive systems and evolution of coastal profiles.

Since all the coastal lengths are considered not finite measures (from [37] onwards) like the lengths in the limit configurations obtained with arc constructions such as (2.1) and (2.14), with Sect. 5 the right time has come to build a bridge towards infinity computing. In fact, the convergence of three current areas of research of great importance like coastal and marine studies, modeling and geometry of iterated systems, and infinity computing, is very promising for a number of upcoming developments.

Sect. 6 finally addresses the conclusions.

In this paper we denote by \mathbb{N} and \mathbb{N}_0 the sets of positive and non-negative integers, respectively. We use the writing \overline{AB} for the line segment with endpoints A and B , $|AB|$ for its length and $\angle ABC$ for the measure of the angle with vertex in B .

2. Iterative systems with circumference arcs

Iterative methods appear in mathematics, geometry, mathematical physics, numerical simulations, etc., in the contexts and in relation to the most varied tools. By sharpening the gaze towards sea waves and coastal profiles, which we will discuss better in Sect. 4, some examples are provided by [20, 28, 40, 56].

This section is devoted to the theoretical foundations of the iterative system employing circumference arcs. The basis is provided, as said in the Introduction, by [23]. Here we try to implement and generalize the setting for our purposes and our needs, also in prevision of future works (see conclusions in Sect. 6).

We begin by summarizing below a list of basic notations and definitions. Let $n_1, n_2, \dots, n_m, \dots$ be a sequence of positive integers and $\mu = i_1, i_2, \dots, i_m$ be an m -dimensional multi-index with $1 \leq i_h \leq n_h$ for all $h = 1, 2, \dots, m$. Let moreover i_{m+1} be a positive integer with $i_{m+1} \leq n_{m+1}$ in analogy with the previous ones and, with reference to Fig. 1, we set:

- let (x_μ, y_μ) be the coordinate of the center of the original arc, or better, of a given arc at level m ;

- $(x_{\mu, i_{m+1}}, y_{\mu, i_{m+1}})$ represents the coordinates of the center of the i_{m+1} -th arc of level $m + 1$ that arises from the i_{m+1} -th part of the original arc;
- R_{μ} is the radius of the original arc;
- $R_{\mu, i_{m+1}}$ is the radius of the i_{m+1} -th derived arc of level $m + 1$;
- $r_{\mu, i_{m+1}}$ is equal to the distance $|(x_{\mu}, y_{\mu}), (x_{\mu, i_{m+1}}, y_{\mu, i_{m+1}})|$;
- Q_{μ} is equal to the distance between the center (x_{μ}, y_{μ}) of an arc of level m and the origin of our reference system, i.e. $Q_{\mu} = |(x_{\mu}, y_{\mu}), (0, 0)|$;
- $Q_{\mu, i_{m+1}}$, in accordance with the previous item, represents the distance $|(x_{\mu, i_{m+1}}, y_{\mu, i_{m+1}}), (0, 0)|$;
- α_{μ} is the measure of the angle relative to the original arc;
- $\alpha_{\mu, i_{m+1}}$ is the measure of the i_{m+1} -th derived arc;
- $\beta_{\mu, i_{m+1}}$ is the measure of the angle correspondent to the i_{m+1} -th piece of the original arc;
- θ_{μ} is measure of the angle (azimuth angle) between the x -axis and the first counterclockwise encountered radius of the original arc;
- $\theta_{\mu, i_{m+1}}$ is the same as θ_{μ} but for the i_{m+1} -th derived arc;
- $\phi_{\mu, i_{m+1}}$ is the measure of the angle between the x -axis and the line through (x_{μ}, y_{μ}) and $(x_{\mu, i_{m+1}}, y_{\mu, i_{m+1}})$;
- $\vartheta_{\mu, i_{m+1}}$ is the measure of the angle between the line through (x_{μ}, y_{μ}) and $(x_{\mu, i_{m+1}}, y_{\mu, i_{m+1}})$ and the radius $R_{\mu, i_{m+1}}$ as in Fig. 2 (a) and (b);
- $\gamma_{\mu, i_{m+1}}$ is the measure of the angle between the radii R_{μ} and $R_{\mu, i_{m+1}}$ as in Fig. 2 (a) and (b);
- ζ_{μ} represents the azimuth angle of the center (x_{μ}, y_{μ}) of an arc of level m with the reference direction (i.e. the angle between the vector from $(0, 0)$ to (x_{μ}, y_{μ}) and the positive x -semiaxis with the usual conventions);
- $\zeta_{\mu, i_{m+1}}$, according to the previous item, is the azimuth angle of $(x_{\mu, i_{m+1}}, y_{\mu, i_{m+1}})$, the center of an arc of level $m + 1$;
- $\Delta := \pi - \phi_{\mu, i_{m+1}}$;
- $s_{\mu, i_{m+1}} := \beta_{\mu, i_{m+1}}/\alpha_{\mu}$ is the *scale reduction* relative to the i_{m+1} -th new arc;
- E_{μ} is the set consisting of the two end points of the arc (of level m) identified by the multi-index μ ;
- $E_m := \bigcup_{\mu \leq (n_1, \dots, n_m)} E_{\mu} = \bigcup_{i_1=1}^{n_1} \bigcup_{i_2=1}^{n_2} \dots \bigcup_{i_m=1}^{n_m} E_{i_1, i_2, \dots, i_m}$ for every integer $m \geq 1$.

We call the set

$$E := \bigcup_{m=1}^{\infty} E_m$$

the *end points set* (or, sometimes, the *limit set* or also the *invariant set*) of the iterative construction. See Proposition 2.1 and its proof for an example of explicit determination of the sets E_m for all $m \geq 1$.

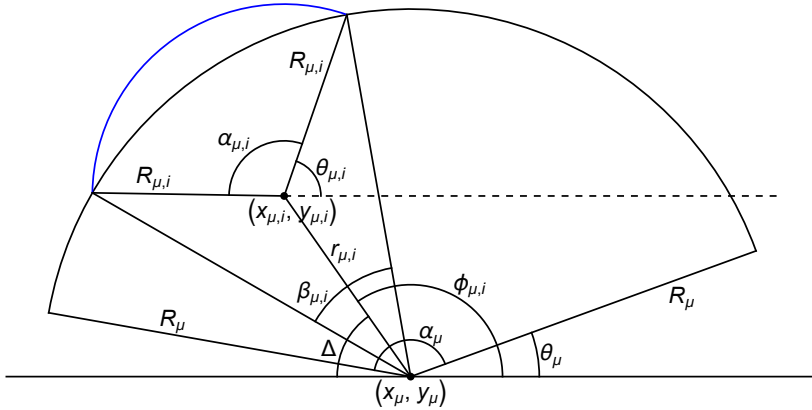


FIGURE 1. A representation of an arc of level m with m -dimensional multi-index $\mu = i_1, i_2, \dots, i_m$. The blue smaller arc is of level $m + 1$ and has multi-index μ, i_{m+1} . In the picture we just use i to mean i_{m+1} to avoid subsuscripts.

The setting described above is completely general and also admits the possibility of starting with any number n_1 of (consecutive) arcs at the first level $m = 1$. Furthermore, it is also possible, with our very general setting, that two m -level arcs, corresponding to multi-indices μ and μ' , are divided in a different number of sub-arcs at the subsequent level $m + 1$. This means that n_{m+1} is the maximum number of subdivisions of an m -level arc and if the number, e.g. n , of $(m + 1)$ -level arcs generated from the m -level arc with multi-index μ, k for $k = n + 1, n + 2, \dots, n_{m+1}$ are null arcs, i.e. $\alpha_{\mu,k} = \beta_{\mu,k} = 0$ for all $k = n + 1, n + 2, \dots, n_{m+1}$.

But in spite of this great generality, for the applications that we want to study closely, we will usually mean consecutive arcs that are generated in equal number n_{m+1} from every arc of level m , and the construction starts from a single given arc of level 1, i.e. assuming $n_1 = 1$.

The recursive equations for an $(m + 1)$ -level arc, also valid in full generality, are given below:

$$\left\{ \begin{array}{l}
x_{\mu, i_{m+1}} = x_{\mu} + \frac{R_{\mu}}{\sin\left(\frac{\alpha_{\mu, i_{m+1}}}{2}\right)} \sin\left(\frac{\alpha_{\mu, i_{m+1}}}{2} + \omega_{\mu, i_{m+1}} \frac{s_{\mu, i_{m+1}} \alpha_{\mu}}{2}\right) \\
\quad \cdot \cos\left(\theta_{\mu} + \sum_{k=1}^{i_{m+1}-1} s_{\mu, k} \alpha_{\mu} + \frac{s_{\mu, i_{m+1}} \alpha_{\mu}}{2}\right), \\
y_{\mu, i_{m+1}} = y_{\mu} + \frac{R_{\mu}}{\sin\left(\frac{\alpha_{\mu, i_{m+1}}}{2}\right)} \sin\left(\frac{\alpha_{\mu, i_{m+1}}}{2} + \omega_{\mu, i_{m+1}} \frac{s_{\mu, i_{m+1}} \alpha_{\mu}}{2}\right) \\
\quad \cdot \sin\left(\theta_{\mu} + \sum_{k=1}^{i_{m+1}-1} s_{\mu, k} \alpha_{\mu} + \frac{s_{\mu, i_{m+1}} \alpha_{\mu}}{2}\right), \\
R_{\mu, i_{m+1}} = \frac{R_{\mu}}{\sin\left(\frac{\alpha_{\mu, i_{m+1}}}{2}\right)} \sin\left(\frac{s_{\mu, i_{m+1}} \alpha_{\mu}}{2}\right), \\
\theta_{\mu, i_{m+1}} = \theta_{\mu} + \sum_{k=1}^{i_{m+1}-1} s_{\mu, k} \alpha_{\mu} + \frac{s_{\mu, i_{m+1}} \alpha_{\mu}}{2} - \frac{a_{\mu, i_{m+1}}}{2} - (1 + \omega_{\mu, i_{m+1}}) \frac{\pi}{2}, \\
\alpha_{\mu, i_{m+1}} = g_{\mu, i_{m+1}}(\alpha_{\mu}),
\end{array} \right. \quad (2.1)$$

where $\omega_{\mu, i_{m+1}} = +1$ or -1 according, respectively, if the orientation of the (μ, i_{m+1}) -th arc is inward or outward with respect to the μ -th arc from which it derives (see Figs. 2(a) and 2(b) below).

For instance, we can consider some simple cases for illustrative purposes.

Example 2.1. One of the simplest possible cases is obtained by starting from

$$\begin{aligned}
n_1 = 1, \quad \alpha_1 = \pi, \quad n_2 = 2 \quad \text{with} \quad \alpha_{1,1} = \alpha_{1,2} = \pi, \\
\beta_{1,1} = \beta_{1,2} = \pi/2 \quad \text{and} \quad \omega_{1,1} = \omega_{1,2} = -1,
\end{aligned} \quad (2.2)$$

and iterating in the same way at each level. This means that, at the generic level $m+1 \geq 2$, we get

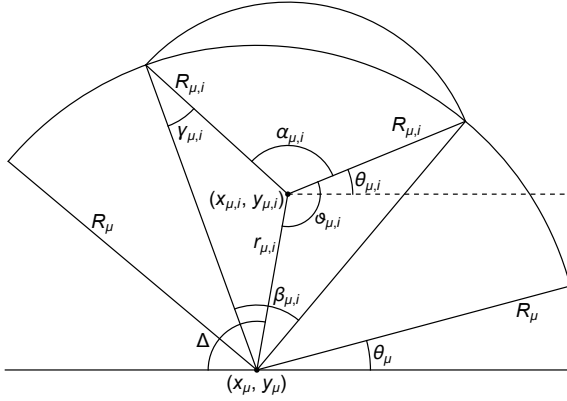
$$n_{m+1} = 2, \quad \alpha_{\mu, k} = \pi, \quad \beta_{\mu, k} = \pi/2 \quad \text{and} \quad \omega_{\mu, k} = -1 \quad \text{for} \quad k = 1, 2, \quad (2.3)$$

where $\mu = i_1, \dots, i_m$ is a multi-index with $i_1 = 1$ and $i_h \in \{1, 2\}$ for all $h = 2, 3, \dots, m$.

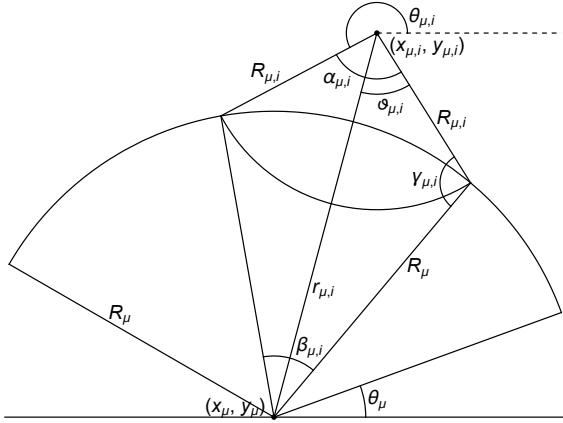
The obtained figures, when m grows, are increasingly better approximations of the *Lévy C curve*, so named for its resemblance to a highly ornate version of the letter C. Instead, if we take in (2.3)

$$\omega_{\mu, k} = (-1)^{i_m+k+1} \quad \text{for all} \quad k = 1, 2 \quad \text{and} \quad m \geq 1, \quad (2.4)$$

we obtain increasing approximations of the *Harter-Heighway dragon*. We point out to the reader that condition (2.4) implies $\omega_{1,1} = -1$ and $\omega_{1,2} = +1$ in (2.2), and in general, at level $m+1$, it produces a total number of 2^{m-2} iterations of the 4-cycle $-1, +1, +1, -1$ for $\omega_{1, i_2, \dots, i_{m+1}}$, where $i_2, i_3, \dots, i_{m+1} \in$



(a) $\omega_{\mu, i_{m+1}} = -1$. This means that the arc of level $m + 1$ with center $(x_{\mu, i_{m+1}}, y_{\mu, i_{m+1}})$ faces outwards with respect to the arc of level m and center (x_{μ}, y_{μ}) from which it originates.



(b) $\omega_{\mu, i_{m+1}} = +1$. This means that the arc with center $(x_{\mu, i_{m+1}}, y_{\mu, i_{m+1}})$ faces inwards with respect to the arc with center (x_{μ}, y_{μ}) which generates it.

FIGURE 2. A representation of the two possible orientations for an arc with multi-index μ, i_{m+1} . The angles $\alpha_{\mu, i_{m+1}}, \theta_{\mu, i_{m+1}}, \vartheta_{\mu, i_{m+1}}$ and $\gamma_{\mu, i_{m+1}}$ are also highlighted in the two cases. As in Fig. 1, i is an abbreviation for i_{m+1} .

$\{1, 2\}$. For instance, at level $m + 1 = 4$ we have

$$\begin{aligned} \omega_{1,1,1,1} &= -1, & \omega_{1,1,1,2} &= +1, & \omega_{1,1,2,1} &= +1, & \omega_{1,1,2,2} &= -1, \\ \omega_{1,2,1,1} &= -1, & \omega_{1,2,1,2} &= +1, & \omega_{1,2,2,1} &= +1, & \omega_{1,2,2,2} &= -1. \end{aligned}$$

Example 2.2. This time we keep the same initial dataset given in (2.2) but with a generic pair of angles $\beta_{1,1} \in]0, \pi[$ and $\beta_{1,2} = \pi - \beta_{1,1}$. The repercussion

in (2.3) is limited only to $\beta_{\mu,1} = \beta_{1,1}$ and $\beta_{\mu,2} = \pi - \beta_{\mu,1} = \beta_{1,2}$ for every multi-index $\mu \in \{1, 2\}^m$ (with $i_1 = 1$, obviously). As $\beta_{1,1}$ varies in $]0, \pi[$ we get a structure similar to the “crown” of every possible *Pythagoras tree*, i.e. the finer details of a generic Pythagoras tree (recall Thales’ theorem on a triangle inscribed in a semicircle).

Example 2.3. Another simple construction can be obtained by starting from

$$\begin{aligned} n_1 = 1, \quad \alpha_1 = \pi, \quad n_2 = 3 \quad \text{with} \quad \alpha_{1,1} = \alpha_{1,2} = \alpha_{1,3} = \pi, \\ \beta_{1,1} = \beta_{1,2} = \beta_{1,3} = \pi/3 \quad \text{and} \quad \omega_{1,1} = \omega_{1,3} = -1, \quad \omega_{1,2} = +1, \end{aligned} \quad (2.5)$$

and iterating this pattern at each level. In this way we obtain, at the generic level $m + 1 \geq 2$,

$$n_{m+1} = 3, \quad \alpha_{\mu,k} = \pi, \quad \beta_{\mu,k} = \pi/3 \quad \text{and} \quad \omega_{\mu,k} = (-1)^k \quad \text{for all } k = 1, 2, 3,$$

where $\mu = i_1, \dots, i_m$ is a multi-index with $i_1 = 1$ and $1 \leq i_h \leq 3$ for all $h = 2, 3, \dots, m$. They are increasingly better approximations of the well known *Sierpiński gasket* or *triangle* (see [9] for its basic version and its d -dimensional generalization).

Example 2.4. Here we consider some easy examples with $\alpha_1 \neq \pi$. Let

$$\begin{aligned} n_1 = 1, \quad \alpha_1 = 2\pi/3, \quad n_2 = 2 \quad \text{with} \quad \alpha_{1,1} = \alpha_{1,2} = 2\pi/3, \\ \beta_{1,1} = \beta_{1,2} = \pi/3 \quad \text{and} \quad \omega_{1,1} = \omega_{1,3} = 1, \end{aligned} \quad (2.6)$$

and we iterate this pattern at every subsequent level. This means that at the level $m + 1 \geq 2$ we get

$$n_{m+1} = 2, \quad \alpha_{\mu,k} = 2\pi/3, \quad \beta_{\mu,k} = \pi/3 \quad \text{and} \quad \omega_{\mu,k} = 1 \quad \text{for } k = 1, 2,$$

where $\mu = i_1, \dots, i_m$ is a multi-index with $i_1 = 1$ and $i_h \in \{1, 2\}$ for all $h = 2, 3, \dots, m$.

Then, when m grows, we obtain increasingly better approximations of the well-known *von Koch curve* (see also [19, 49]).

Example 2.5. Starting from the data chosen in (2.6) for the main parameters, we now modify them as follows

$$\begin{aligned} n_1 = 1, \quad \alpha_1 = 17\pi/18, \quad n_2 = 2 \quad \text{with} \quad \alpha_{1,1} = \alpha_{1,2} = 17\pi/18, \\ \beta_{1,1} = \beta_{1,2} = 17\pi/36 \quad \text{and} \quad \omega_{1,1} = \omega_{1,2} = 1, \end{aligned}$$

and iterate at each level m . In this way, at the generic level $m + 1 \geq 2$, we obtain

$$n_{m+1} = 2, \quad \alpha_{\mu,k} = 17\pi/18, \quad \beta_{\mu,k} = 17\pi/36 \quad \text{and} \quad \omega_{\mu,k} = 1 \quad \text{for } k = 1, 2,$$

where $\mu = i_1, \dots, i_m$ is a multi-index with $i_1 = 1$ and $i_h \in \{1, 2\}$ for every $h = 2, 3, \dots, m$.

Note that $17\pi/18 = 2 \cdot 85^\circ$. Therefore, as the level m increases, we obtain better and better approximations of the fractal curve known as *Cesàro fractal* 85° or *Cesàro triangle*, or also as *von Koch curve* 85° (see [38, 27]). It is a variation of the (standard) von Koch curve considered in Example 2.4, whose distinctive angle is 60° .

At the end of this short set of examples, we want to point out to the reader how the resulting sets from an arc system have, obviously, different fractal dimensions in general. In the simplest case in which the same number of identical arcs are always generated from each arc of each level, the fractal dimension of the limit set E obtained from the construction can be easily calculated. More precisely, considering an arc-based system \mathcal{S} with

$$\begin{aligned} n_1 = 1, \quad n_2 = n_3 = \dots = n_h = \dots = n \geq 2, \\ \alpha_\mu = \alpha_1 \leq \pi \text{ and } \beta_\mu = \alpha_1/n \text{ for all multi-index } \mu \text{ of level } m \geq 2, \end{aligned} \quad (2.7)$$

then the fractal dimension of $E(\mathcal{S})$ is given by the following formula

$$\dim(E(\mathcal{S})) = \frac{\ln n}{\ln \left(\frac{\sin(\alpha_1/2)}{\sin(\alpha_1/2n)} \right)}. \quad (2.8)$$

The previous formula is simple to prove using, for instance, the box-counting dimension (see [23]).

For example, using (2.8) we can easily compute the fractal dimension of the Cesàro fractal C obtained in Example 2.5,

$$\dim(C) = \frac{\ln 2}{\ln \left(\frac{\sin(17\pi/36)}{\sin(17\pi/72)} \right)}, \quad (2.9)$$

which is equal to the more common writing $\ln 4 / \ln(2 + 2 \cos(17\pi/36)) \approx 1.7848241$. As further examples, for the von Koch curve K , the Sierpiński gasket G and the Lévy C curve L of Examples 2.4, 2.3 and 2.1, respectively, we find the following well-known values

$$\begin{aligned} \dim(K) &= \frac{\ln 2}{\ln \left(\frac{\sin(\pi/3)}{\sin(\pi/6)} \right)} = \frac{\ln 2}{\ln \sqrt{3}} = \log_3 4 \approx 1.2618595, \\ \dim(G) &= \frac{\ln 3}{\ln \left(\frac{\sin(\pi/2)}{\sin(\pi/6)} \right)} = \frac{\ln 3}{\ln 2} = \log_2 3 \approx 1.5849625, \\ \dim(L) &= \frac{\ln 2}{\ln \left(\frac{\sin(\pi/2)}{\sin(\pi/4)} \right)} = \frac{\ln 2}{\ln \sqrt{2}} = \log_{\sqrt{2}} 2 = 2. \end{aligned}$$

In cases more general than (2.7) formula (2.8) no longer hold. Then the fractal dimension can be investigated case by case, trying to use one of the usual techniques (see, e.g. [19]). But it may also even happen that the end points set E of an arc system is not a fractal at all, as the following result shows.

Consider the arc system generated by the following initial data

$$\begin{aligned} n_1 = 1, \quad \alpha_1 = 3\pi/2, \quad n_2 = 3 \text{ with } \alpha_{1,1} = \alpha_{1,2} = \alpha_{1,3} = 3\pi/2, \\ \beta_{1,1} = \beta_{1,2} = \beta_{1,3} = \pi/2 \quad \text{and} \quad \omega_{1,1} = \omega_{1,2} = \omega_{1,3} = -1. \end{aligned} \quad (2.10)$$

At the generic level $m + 1 \geq 2$ we get

$$n_{m+1} = 3, \quad \alpha_{\mu,k} = 3\pi/2, \quad \beta_{\mu,k} = \pi/2 \quad \text{and} \quad \omega_{\mu,k} = -1 \quad \text{for} \quad k = 1, 2, 3, \quad (2.11)$$

where $\mu = i_1, i_2, \dots, i_m$ is an m -dimensional multi-index with $i_1 = 1$ and $i_h \in \{1, 2, 3\}$ for every $h = 2, 3, \dots, m$.

Proposition 2.1. *Let \mathcal{S} be the arc-based system whose levels are given by (2.10) and (2.11). Then we have*

$$E_m(\mathcal{S}) = \begin{cases} \{(1, 0), (0, -1)\} & \text{if } m = 1, \\ \{(1, 0), (0, 1), (-1, 0), (0, -1)\} & \text{if } m = 2, \\ \{(a, b) \in [1 - m \dots m - 1]^2 : a \not\equiv b \pmod{2} \\ \text{and } a - b \neq m - 3\} & \text{if } m \geq 3, \end{cases} \quad (2.12)$$

and, for the end points set of \mathcal{S} , we find

$$E(\mathcal{S}) = \{(a, b) \in \mathbb{Z}^2 : a \not\equiv b \pmod{2}\}. \quad (2.13)$$

Proof. Firstly we recall that $[a \dots b]$ is the usual notation for discrete intervals, i.e. $[a \dots b] := [a, b] \cap \mathbb{Z}$ for any integers $a \leq b$.

Determining $E_m(\mathcal{S})$ for the first three occurrences is trivial. Then, to prove (2.12) in full, we can use an inductive argument on $m \geq 3$, noting how the inductive step from level m to level $m + 1$ creates a border all around the set $E_m(\mathcal{S})$.

Finally, (2.13) is an immediate consequence of (2.12). \square

From the previous proposition we deduce that $E(\mathcal{S})$ has fractal dimension zero, and so it is not a fractal (in fact, it is a square lattice). It is therefore important to point out that the end points set E of an arc-based system is not necessarily a fractal, in general.

We conclude this section by finding polar recursive equations for a general arc system. Going directly to the final results, in polar coordinates the equations in (2.1), mainly depending on $\alpha_{\mu, i_{m+1}}$, $\beta_{\mu, i_{m+1}}$, $\omega_{\mu, i_{m+1}}$ and R_μ , θ_μ , can be written as follows

$$\left\{ \begin{array}{l}
 Q_{\mu, i_{m+1}} = Q_{\mu} + \frac{R_{\mu}}{\sin\left(\frac{\alpha_{\mu, i_{m+1}}}{2}\right)} \sin\left(\frac{\alpha_{\mu, i_{m+1}}}{2} + \omega_{\mu, i_{m+1}} \frac{s_{\mu, i_{m+1}} \alpha_{\mu}}{2}\right) \cos\left(\theta_{\mu} + \sum_{k=1}^{i_{m+1}-1} s_{\mu, k} \alpha_{\mu} + \frac{s_{\mu, i_{m+1}} \alpha_{\mu}}{2} - \zeta_{\mu}\right), \\
 \zeta_{\mu, i_{m+1}} = \frac{\pi}{2} + \left[1 - 2\chi_{\mathbb{R}_0^+} \left(\frac{R_{\mu}}{\sin\left(\frac{\alpha_{\mu, i_{m+1}}}{2}\right)} \sin\left(\frac{\alpha_{\mu, i_{m+1}}}{2} + \omega_{\mu, i_{m+1}} \frac{s_{\mu, i_{m+1}} \alpha_{\mu}}{2}\right) \cos\left(\theta_{\mu} + \sum_{k=1}^{i_{m+1}-1} s_{\mu, k} \alpha_{\mu} + \frac{s_{\mu, i_{m+1}} \alpha_{\mu}}{2}\right) + Q_{\mu} \cos(\zeta_{\mu}) \right) \right] \\
 \cdot \left[\frac{\pi}{2} - \arcsin \left(\frac{\frac{R_{\mu}}{\sin\left(\frac{\alpha_{\mu, i_{m+1}}}{2}\right)} \sin\left(\frac{\alpha_{\mu, i_{m+1}}}{2} + \omega_{\mu, i_{m+1}} \frac{s_{\mu, i_{m+1}} \alpha_{\mu}}{2}\right) \sin\left(\theta_{\mu} + \sum_{k=1}^{i_{m+1}-1} s_{\mu, k} \alpha_{\mu} + \frac{s_{\mu, i_{m+1}} \alpha_{\mu}}{2}\right) + Q_{\mu} \sin(\zeta_{\mu})}{Q_{\mu} + \frac{R_{\mu}}{\sin\left(\frac{\alpha_{\mu, i_{m+1}}}{2}\right)} \sin\left(\frac{\alpha_{\mu, i_{m+1}}}{2} + \omega_{\mu, i_{m+1}} \frac{s_{\mu, i_{m+1}} \alpha_{\mu}}{2}\right) \cos\left(\theta_{\mu} + \sum_{k=1}^{i_{m+1}-1} s_{\mu, k} \alpha_{\mu} + \frac{s_{\mu, i_{m+1}} \alpha_{\mu}}{2} - \zeta_{\mu}\right)} \right) \right], \\
 R_{\mu, i_{m+1}} = \frac{R_{\mu}}{\sin\left(\frac{\alpha_{\mu, i_{m+1}}}{2}\right)} \sin\left(\frac{s_{\mu, i_{m+1}} \alpha_{\mu}}{2}\right), \\
 \theta_{\mu, i_{m+1}} = \theta_{\mu} + \sum_{k=1}^{i_{m+1}-1} s_{\mu, k} \alpha_{\mu} + \frac{s_{\mu, i_{m+1}} \alpha_{\mu}}{2} - \frac{a_{\mu, i_{m+1}}}{2} - (1 + \omega_{\mu, i_{m+1}}) \frac{\pi}{2}, \\
 \alpha_{\mu, i_{m+1}} = g_{\mu, i_{m+1}}(\alpha_{\mu}),
 \end{array} \right. \tag{2.14}$$

where $\chi_{\mathbb{R}_0^+}$ is the *characteristic function* of \mathbb{R}_0^+ which maps a non-negative real number to 1 and a negative one to 0.

3. Replacing arcs with other curves: towards more general cases

3.1. Universality of the arc system for iterated bisections

It is interesting to replace arcs with other types of curves, even very generic ones. But extensive research in this direction is beyond the scope of this paper. Here we only point out a “universal” property of the system with arcs: replacing the arcs with any type of curve, if $n_h \leq 2$ for each level $h = 1, 2, 3, \dots$, then both the figure obtained at a generic level m and the limit figure can be obtained with an arc construction as in Sect. 2 (remember in particular Eqs. (2.1) and (2.14)), suitably choosing the arcs from time to time, at each level. If, on the other hand, we have $n_h \geq 3$ for some $h \geq 2$ ($n_1 \geq 3$ doesn’t matter much), the above statement is no longer true, unless we seriously alter the correspondence of the levels. To explain this better let us consider the enlightening case where $n_h \leq 2$ definitively, i.e. for each h greater than a certain fixed level m . In fact, in this case, we could add a finite number of extra levels to the arc construction and obtain the same result, but by altering the correspondence between levels in the two constructions. These statements could be formulated in a precise and formal way, and demonstrated, but due to the many and heavy notations we would lose sight of the purposes of the paper and the initial applications to real coast models. We will explore these topics in detail in a future paper with a more geometric approach.

In the next Subsect. 3.2 we begin to discuss some cases involving logarithmic spirals.

3.2. The case of the logarithmic spiral

The logarithmic spiral, among the many existing types of spirals (for example, Archimedean, hyperbolic, parabolic, etc.), has many particularly interesting properties such as those of constant slope angle and self-similarity, i.e. a scaled copy of it is congruent to the original curve through a rotation. Precisely because of the fascinating and unique property of self-similarity, the logarithmic spiral was called *spira mirabilis* by Jacob Bernoulli who even wanted it on his tomb.

As well known, the polar equation of a *logarithmic spiral* is of the type

$$r(\theta) = ae^{b\theta} \quad (3.1)$$

with a and b real parameters, $a > 0$. The term b is often called the *growth constant*. If $b = 0$ in (3.1) we simply obtain a circumference of radius a , instead, if $b = 2\pi^{-1} \ln \varphi$ (and $a = 1$) we obtain the polar equation of the *golden spiral* (with initial radius 1),

$$r(\theta) = e^{\frac{2\theta}{\pi} \ln \varphi}, \quad (3.2)$$

where $\varphi = \frac{1+\sqrt{5}}{2}$ is the *golden section*. This special logarithmic spiral has the propriety that it grows by a factor φ with every quarter turn. The spiral \mathcal{P} constructed with quarter-circle arcs having radius equal to the integer powers (positive and negative) of φ , i.e.

$$\dots, \varphi^{-n}, \dots, \varphi^{-3}, \varphi^{-2}, \varphi^{-1}, 1, \varphi^1, \varphi^2, \varphi^3, \dots, \varphi^n, \dots,$$

approximates the golden spiral very well, and is also self-similar. The *Fibonacci spiral* \mathcal{F} is instead constructed with quarter-circle arcs having radius determined by the homonymous sequence

$$\{F_n\}_{n \in \mathbb{N}} = \{1, 1, 2, 3, 5, 8, 13, 21, 34, \dots\},$$

where $F_0 = 0$ is not influential. For very large n the spiral \mathcal{F} approximates \mathcal{P} very well, and therefore, as n approaches infinity, \mathcal{F} approximates the golden spiral itself well. For more details and new geometric constructions based on Fibonacci numbers, the interested reader can see [11, 12, 53] and the references therein. Instead in [2] the authors exploit a chain of triangles to describe logarithmic spirals and in particular consider the golden spiral, the *spira solaris* and *Pheidia spiral*. The last two are usually obtained by choosing the growth constant $b = \pi^{-1} \ln \varphi$ and $b = (2\pi)^{-1} \ln \varphi$, respectively, and $a = 1$ in Eq. (3.1).

Example 3.1. Let us consider as an example a system not based on arcs of circumference but on the following arc of the golden spiral (with initial radius 1):

$$r(\theta) = e^{2\theta\pi^{-1} \ln \varphi}, \quad \theta \in [0, \pi]. \quad (3.3)$$

It starts at the point $A = (1, 0)$, passes through the point $C = (0, \varphi)$ and ends at $E = (-\varphi^2, 0)$. At the second level of our new system based on the golden spiral arc (3.3), we consider the two line segments \overline{AC} and \overline{CE} as in

Fig. 3 and we draw two spiral arcs similar to (3.3) on them, scaled by the factor

$$\frac{\sqrt{2+\varphi}}{2+\varphi} \quad \text{and} \quad \frac{\varphi\sqrt{2+\varphi}}{2+\varphi},$$

respectively.¹ C is a very special point because it is the only point on the arc (3.3) such that $\angle ACE = \pi/2$, i.e. ACE is a right angle. Then we can consider an arc system starting from the following data at level $m = 1$:

$$x_1 = -\frac{\varphi}{2}, \quad y_1 = 0, \quad R_1 = 1 + \frac{\varphi}{2} \quad \text{and} \quad \alpha_1 = \pi. \quad (3.4)$$

At level $m = 2$ we generate two smaller arcs by choosing (see Fig. 4)

$$(x_{1,1}, y_{1,1}) = \left(\frac{1}{2}, \frac{\varphi}{2}\right), \quad R_{1,1} = \frac{\sqrt{2+\varphi}}{2}, \quad r_{1,1} = \frac{\sqrt{3+4\varphi}}{2}, \quad (3.5)$$

$$\alpha_{1,1} = \pi, \quad \beta_{1,1} = \arctan(2), \quad \omega_{1,1} = -1,$$

and

$$(x_{1,2}, y_{1,2}) = \left(-\frac{1+\varphi}{2}, \frac{\varphi}{2}\right), \quad R_{1,2} = r_{1,1}, \quad r_{1,2} = R_{1,1}, \quad (3.6)$$

$$\alpha_{1,2} = \pi, \quad \beta_{1,2} = \pi - \arctan(2), \quad \omega_{1,2} = -1.$$

It is now clear that the system obtained by iterating the construction in Fig. 3, with golden spiral arcs similar to (3.3), produces the same set for m approaching infinity as the arc system obtained by iterating (3.5) and (3.6). It is a particular case of Example 2.2, and the limit figure is the “crown” of a Pythagoras three.

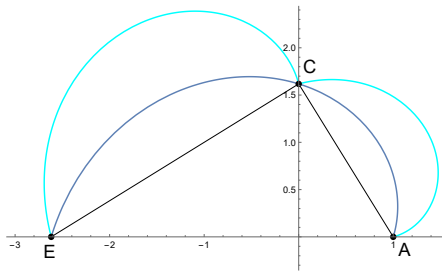


FIGURE 3. The golden spiral arc (3.3) and two similar smaller copies in cyan drawn on \overline{AC} and \overline{CE} , whose centers are $((2+\varphi)/5, (2\varphi-1)/5)$ and $(-(2+\varphi)/5, (1+3\varphi)/5)$, respectively.

Example 3.2. As in Example 3.1 we consider a system based on the golden spiral arc (3.3). The first level in this system is the same as in the previous example, but at the second level, $m = 2$, we consider the point $B = (\sqrt{\varphi/2}, \sqrt{\varphi/2})$ obtained for an angle $\theta = \pi/4$, instead of $C = (0, \varphi)$. Then

¹The reader should always keep in mind the relation $\varphi^2 = \varphi + 1$.

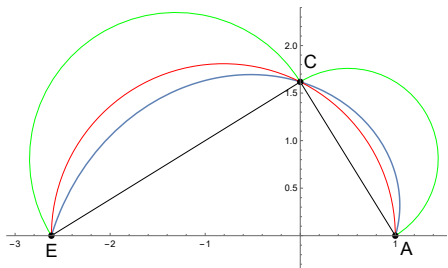


FIGURE 4. The circumference arc (3.4) represented in red with the two smaller copies given by (3.5) and (3.6) in green.

we take the two line segments \overline{AB} and \overline{BE} as in Fig. 5 and we construct on them two spiral arcs similar to (3.3), scaled by a factor

$$\frac{\sqrt{1 + \varphi - \sqrt{2\varphi}}}{2 + \varphi} = \sqrt{\frac{1 + (\varphi - 2)\sqrt{2\varphi}}{5}} \quad (3.7)$$

and

$$\frac{\sqrt{2 + 4\varphi + (1 + \varphi)\sqrt{2\varphi}}}{2 + \varphi} = \sqrt{\frac{2\varphi + \sqrt{2\varphi}}{5}}, \quad (3.8)$$

respectively. The correspondent centers of the spirals are

$$\left(\frac{2 + \varphi}{5} + \frac{3 - \varphi}{5} \sqrt{\frac{\varphi}{2}}, \sqrt{\frac{\varphi - 1}{10}} \right) \quad (3.9)$$

and

$$\left(\frac{2 + \varphi}{5} \left(\sqrt{\frac{\varphi}{2}} - 1 \right), \sqrt{\frac{\varphi}{2}} - \sqrt{\frac{\varphi - 1}{10}} \right), \quad (3.10)$$

respectively. This system based on the spiral arc (3.3) continues iteratively by considering the points B' and B'' belonging to the spiral arcs on \overline{AB} and \overline{BE} respectively, and correspondent to B on the original spiral arc (3.3). We get

$$B' = \left(\frac{1 + \varphi + \sqrt{2\varphi}}{2 + \varphi}, \frac{-\varphi + \sqrt{2\varphi}}{2 + \varphi} \right)$$

and

$$B'' = \left(\frac{(1 + \varphi)(-1 + \sqrt{2\varphi})}{2 + \varphi}, \frac{\varphi + (1 + \varphi)\sqrt{2\varphi}}{2 + \varphi} \right).$$

Then, for the level $m = 3$, we consider the four line segments $\overline{AB'}$, $\overline{B'B}$, $\overline{BB''}$ and $\overline{B''E}$, and we construct four spiral arcs similar to (3.3) and so on.

Now we go back to considering a standard system (2.1) based on circumference arcs. At the level $m = 1$ it starts from the following data:

$$n_1 = 1, \quad \alpha_1 = \pi + 2 \arctan \left(\frac{\varphi - \sqrt{2(\varphi - 1)}}{2 + \varphi} \right), \quad (3.11)$$

$$R_1 = \sqrt{1 + 2\varphi - \frac{\varphi\sqrt{2(\varphi - 1)}}{2}}.$$

At the second level ($m = 2$) we use

$$n_2 = 2, \quad \alpha_{1,1} = \alpha_{1,2} = \alpha_1, \quad \omega_{1,1} = \omega_{1,2} = -1,$$

$$\beta_{1,1} = 2 \arctan \left(\sqrt{\frac{10 + 15\varphi + (1 + 2\varphi)(2\sqrt{2(\varphi - 1)} - 4\sqrt{2\varphi})}{58 + 89\varphi}} \right)$$

$$\approx 0.500689403,$$

$$\beta_{1,2} = 2 \arctan \left(\sqrt{11 + 18\varphi + 2 \frac{(11 + 18\varphi)\sqrt{2\varphi} + (7 + 11\varphi)\sqrt{2(\varphi - 1)}}{5}} \right)$$

$$\approx 2.918945111. \quad (3.12)$$

The arc system continues iteratively in the obvious way, getting at the generic level $m + 1 \geq 3$:

$$n_m = 2, \quad \alpha_{\mu,1} = \alpha_{\mu,2} = \alpha_\mu, \quad \omega_{\mu,1} = \omega_{\mu,2} = -1,$$

$$\beta_{\mu,1} = \beta_{1,1} \quad \text{and} \quad \beta_{\mu,2} = \beta_{1,2},$$

where $\mu = i_1, \dots, i_m$ is, as usual, an m -dimensional multi-index. To facilitate the visualization we can take the center of the first arc (3.11) in

$$O' = (x_1, y_1) = \left(\frac{-\varphi}{2}, \frac{\varphi - \sqrt{2(\varphi - 1)}}{2} \right) \quad (3.13)$$

instead of in the origin; this means that the circumference arc (3.11) passes through the points A , B and E , as Fig. 6 shows. It is clear that at level $m = 2$ the conditions in (3.12) construct on the line segments \overline{AB} and \overline{BE} two arcs similar to the arc through A , B , E shown in Fig. 6, but scaled by the factors given in (3.7) and (3.8), respectively.

The limit figure obtained from this arc system is very different from the one obtained in Example 3.1: the point B was in fact specifically chosen for this purpose. Note, first of all, that the factor in (3.8) is greater than 1, more precisely

$$\sqrt{\frac{2\varphi + \sqrt{2\varphi}}{5}} \approx 1.003491447.$$

This means that the limit figure expands towards infinity unrolling, in a certain sense, from the point E . However, we will not do here in-depth convergence studies from a topological point of view because this would take us away from the objectives of this paper.

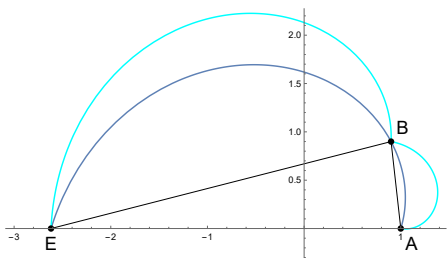


FIGURE 5. The golden spiral arc given in (3.3) and two similar smaller copies constructed on the line segments \overline{AB} and \overline{BE} , whose centers are given in (3.9) and (3.10), respectively.

4. Applications to coastal morphology

In the previous two sections we have tried to lay the foundations of a suitable and effective mathematical framework to be applied, among many possible things, to the study of coastal profiles.

In the study of coastal profiles from a mathematical point of view, a real turning point occurred in the last century when what now goes by the name of “the coastline paradox” became more and more clear: any landmass of the terraqueous globe it trivially has a finite surface, however, in a completely counterintuitive way, the length of its coastline is infinite. The first statement in this sense is contained in [51], but the more in-depth studies began from the already mentioned [37] onwards.

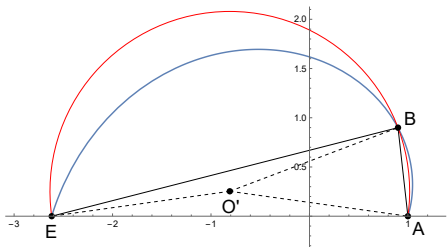


FIGURE 6. A circumference arc through A, B, E with center O' given by (3.13) represents the first level of the arc system (2.1) in the considered case.

One of the first mathematical models on coastlines to be theorized and studied concerns the headland-bay beaches, as announced in the Introduction. It starts from the numerous observations on the concurrence of promontories, often rocky or of higher land, and a bay with a rather characteristic shape sometimes on one side, sometimes on both. It is very relevant that studies of various types go back up to about two hundred years ago (see [6] by Sir Henry T. De la Beche dating back to 1833 and see [8] for an interesting historical account that recalls numerous sources), but the first model that described this type of coastal conformation in a mathematically satisfactory way is found in [55] which presents the so-called *logarithmic spiral model*. Subsequently, many articles have adopted this basic model, of which [26, 32] and [52] are among the best known.

A second main model for HBB, the *parabolic model*, was presented in 1989 through [21]. In recent years this model has found many applications and developments; see for example [1, 7, 31, 35, 36].

The *hyperbolic tangent model*, the last of the three best known and validated models for HBB (see also [31] for an easy summary on all three), was introduced in 1999 by [39]. Among the latest researches based on the parabolic model for HBBs we mention [16, 29, 30, 36].

Another model, different from the three best known ones mentioned above, has recently been proposed in [34]. It is a very simple model of elliptical type. The same article compares the three traditional models with the new elliptical one on some real HBBs.

Finally, we inform the reader that two years ago, in 2021, a voluminous monograph completely dedicated to HBBs was also published (see [22], about 800 pages).

Many other studies on the evolution of coastal profiles on a long-term time scale can be found in the review [54] and its bibliography. Furthermore, more recently several papers have been published on the problem of trying to predict the evolution of coastal profiles. For example, equilibrium-based models [17], diffusion type models [4, 5, 25], grid-based approaches [41], vector-based coastline models [24, 43], and many others.

Returning to consider HBBs, the literature in this case often deals with problems of applicability of the three main models of HBBs, and others related to errors, approximations and distortions between the model and real physical profiles. In [7], for example, the authors go precisely in this direction trying to highlight the limits of applicability of the existing models. In the case of the logarithmic spiral model, to give another example, sometimes there are notable differences between what the model can describe near the center of the spiral and in the farthest part from it; in fact, precisely by moving towards the least curved part of the spiral, divergences frequently emerge which cannot be filled in any way. Similar applicability issues, in particular regarding the positioning of the control points for the parabolic model, uncertainty, deviations and distortions, are studied in [29] and [30].

The mathematical framework and tools described in this work, among the many possible applications as well as the many possible reflections also in pure mathematics, are also intended to improve the existing models for HBBs. As mentioned above, often a single logarithmic spiral or a single ellipse is not enough to outline the profile of a HBB, unless there are considerable errors or alterations. The mathematical framework outlined here allows the introduction of “multiple logarithmic spiral” models, “multiple ellipse” models, etc. These models, based on what is set out in Sects. 2 and 3, can use a number of arcs of curve, spiral, ellipse, etc., variable according to the degree of precision desired, which can be represented by the level m . In this way, taking $n_1 = 1$, at the level $m = 1$ one would have one of the classic logarithmic spiral, hyperbolic tangent, parabolic or elliptical models mentioned above. At higher levels $m \geq 2$, increasingly more precise mathematical descriptions would be obtained. A multiple spiral or multiple ellipse model, etc., also finds support from a geomorphological point of view, especially in the case of significant geo-structural inhomogeneities in the HBB system. For example, in the event that different morphological consistencies, sediment or rock densities, different heights of the beach and dunes present therein, different depths of the seabed, etc. occur or alternate, then several HBBs systems or subsystems can be configured at the interior of a major or principal one. Furthermore, given the fractal nature of coastlines (remember [37]), this fits perfectly with the existence, at least theoretically, of any possible level $m \in \mathbb{N}$ of representation and approximation.

The arc-fractal system is also used in [23] to describe the dynamical evolution of coastal profiles. The basic assumptions are those that the dynamics of the coastline, at least in some parts of the world, is governed only by the phenomena of erosion due to sea waves and sedimentation. This is true at least for part of the coasts, but not for all because other non-negligible phenomena often occur such as currents along the coastline and the consequent transport of sediments.

Systems such as those described by Eqs. (2.1) and (2.14), or those based on other elementary curves (such as the golden spiral, recall Examples 3.1 and 3.2) or on completely general curves, are capable of interpreting the temporal evolution of a coastline, where the increase of the level m represents a discrete set of sequential instants in time. Considering a certain level $m \in \mathbb{N}$, each of the n_{m+1} curves that appear at the following level, roughly speaking, can be inserted in two ways given by the reflection along the straight line joining the extreme points (this corresponds to the two possibilities $\omega_{\mu,i} = \pm 1$ in the case of arcs, see Sect. 2). By randomly choosing the reflections, very jagged curves are generated when m increases, and they are very similar to natural coastal profiles. In Fig. 7, for example, golden spiral arcs and randomized reflections have been used.

The limit figure that would be obtained for m tending to infinity in constructions like those of Fig. 7, is obviously a fractal (or rather, a random



FIGURE 7. A curve obtained by random reflections of golden spiral arcs at level $m = 18$.

fractal). We will address the connections to the mathematics of infinity and infinity computing in the following section.

5. Lengths, levels and infinity computing

This section is devoted to presenting and highlighting some interesting connections between recursive systems based on arcs such as (2.1), (2.14), or other more general ones discussed in Sect. 3, and new numerical-computational systems which allow in particular a numerical quantification of infinite quantities. We recall that we have as concrete objective, also for future works, the development of models and applications to the morphology of coastal profiles, then the possibility of using some of the newest numerical-computational systems, very much in vogue today, which allow in particular a precise evaluation of infinite lengths through proper and explicit numbers appears very useful and advantageous. In fact, while Mandelbrot's famous work [37] on the length of the British coast appeared in 1967 as a breaking paper, today it is quite obvious and accepted by all, the fact that any stretch of real coast, even short and apparently rectilinear, has, if we want to be formally and rigorously exact, an infinite length value. Therefore, to measure real stretches of coast in a precise way, and above all to compare them with each other, the numerical system of the reals is, at least in theory and in principle, absolutely insufficient and unsuitable. Today there are many possible modern systems (and less modern ones²) which address similar problems through a different mathematical approach from the classical one deriving from conventional mathematical analysis headed by Weierstrass and Cauchy. Among them we recall the *non-standard analysis* introduced by Robinson, whose most famous work [42] is significantly contemporary (1966) to the article by Mandelbrot just quoted. To take advantage of an extensive and commented bibliography on the state of the art on unconventional number systems, we refer the reader to the introduction of [15] and to the references contained therein.

²Let us remember that the notion of *infinitesimal* was foundational and omnipresent in the *infinitesimal calculus* of Leibnitz, a name that mathematical analysis often continued to maintain throughout the 20th century.

Among such many possible options we choose to use the ease of approach of the system introduced by Sergeev in the early years of the current century, based on the fundamental unit $\textcircled{1}$ for infinite numbers, called *grossone*. For introductory essays we refer the reader to [48, 50]. Applications and connections with fractals and space filling curves can be found in [3, 9, 10, 47, 49], with the interesting concept of “blinking fractals” in [14, 45]. Direct applications to spirals are contained in [46] and for the Infinity Computer, linked to grossone, the reader can see [18] and the references therein.

5.1. Levels and lengths

We start by considering the length of the curve obtained by a general arc construction whose recursive equations are those in (2.1). For the second level, for instance, we get

$$l(2) = \sum_{i_1=1}^{n_1} \sum_{i_2=1}^{n_2} R_{i_1, i_2} \alpha_{i_1, i_2}.$$

This is generalized at level m by

$$l(m) = \sum_{i_1=1}^{n_1} \sum_{i_2=1}^{n_2} \dots \sum_{i_m=1}^{n_m} R_{i_1, i_2, \dots, i_m} \alpha_{i_1, i_2, \dots, i_m} \quad (5.1)$$

or, using the multi-index notation,

$$l(m) = \sum_{\mu \leq (n_1, \dots, n_m)} R_\mu \alpha_\mu. \quad (5.2)$$

Recalling the explicit constructions seen in Sect. 2, let now L_m be the curve obtained in Example 2.1 at level m , i.e. the approximation of Lévy C curve through arc construction at level m . It is immediate from (5.2) that the following formulas hold for its length $l(L_m)$:

$$l(L_1) = R_1 \pi, \quad l(L_{m+1}) = 2 \frac{\sqrt{2}}{2} l(L_m) \quad \text{for all } m \geq 1, \quad (5.3)$$

and then

$$l(L_m) = \left(\sqrt{2}\right)^{m-1} R_1 \pi \quad (5.4)$$

for all $m \geq 1$. Obviously, for the approximations H_m of the Harter-Heighway dragon, formulas completely equal to (5.3) and (5.4) hold. Instead, for the approximations G_m , $m \in \mathbb{N}$, of the Sierpiński gasket shown in Example 2.3, we get from (5.2)

$$l(G_1) = R_1 \pi, \quad l(G_{m+1}) = \frac{3}{2} l(G_m)$$

and

$$l(G_m) = \left(\frac{3}{2}\right)^{m-1} R_1 \pi \quad (5.5)$$

for all $m \geq 1$.

Remark 5.1. It would be very interesting to study less obvious measures related to the structures L_m , H_m , G_m , etc. For example the length of the right and left boundary of L_m , the area enclosed by L_m , etc; but this would be beyond the scope of the present work. On the other hand, in case of using a Lindenmayer system to construct the Lévy C curve, see instead [44].

We denote by K_m the curve of level m obtained in Example 2.4, whose limit generates the von Koch curve K . From (5.2) we get

$$l(K_1) = R_1 \frac{2}{3} \pi, \quad l(K_{m+1}) = \frac{2}{\sqrt{3}} l(K_m)$$

and

$$l(K_m) = \frac{2^m}{3^{(m+1)/2}} R_1 \pi \quad (5.6)$$

for all $m \geq 1$.

Similarly we denote by C_m the curve of level m constructed in Example 2.5: its limit for $m \rightarrow \infty$ yields the Cesàro fractal 85° already denoted by C in (2.9). Using (5.2) in this case as well, we obtain

$$l(C_1) = R_1 \frac{17}{18} \pi, \quad l(C_{m+1}) = 2 \frac{\sin(19\pi/72)}{\cos(\pi/36)} l(C_m)$$

and

$$l(C_m) = \frac{17 \cdot 2^{m-2}}{9} \left(\frac{\sin(19\pi/72)}{\cos(\pi/36)} \right)^{m-1} R_1 \pi \quad (5.7)$$

for all positive integer m .

Referring now to Example 2.2 let us set, to simplify the notations, $\beta = \beta_{1,1} \in]0, \pi[$. We denote by $P_{\beta,m}$ the curve obtained at level $m \geq 1$ through the arc construction as done in Example 2.2 just mentioned, i.e. starting from (2.2) but with generic $\beta = \beta_{1,1}$. Note that if $\mu = i_1, \dots, i_m$ is as usual an m -dimensional multi-index with $m \geq 1$, then

$$R_{\mu,1} = \sin\left(\frac{\beta}{2}\right) R_\mu \quad \text{and} \quad R_{\mu,2} = \cos\left(\frac{\beta}{2}\right) R_\mu. \quad (5.8)$$

From (5.2) and (5.8) we get $l(P_{\beta,1}) = R_1 \pi$ and

$$\begin{aligned} l(P_{\beta,m+1}) &= \sum_{\substack{\mu \leq (1,2,\dots,2) \\ i_{m+1} \leq 2}} R_{\mu,i_{m+1}} \pi \\ &= \sum_{\mu \leq (1,2,\dots,2)} \left(\sin\left(\frac{\beta}{2}\right) + \cos\left(\frac{\beta}{2}\right) \right) R_\mu \pi \\ &= \left(\sin\left(\frac{\beta}{2}\right) + \cos\left(\frac{\beta}{2}\right) \right) \sum_{\mu \leq (1,2,\dots,2)} R_\mu \pi \\ &= \left(\sin\left(\frac{\beta}{2}\right) + \cos\left(\frac{\beta}{2}\right) \right) l(P_{\beta,m}) \end{aligned}$$

for all $m \geq 1$. Then, by induction we conclude that

$$l(P_{\beta,m}) = \left(\sin\left(\frac{\beta}{2}\right) + \cos\left(\frac{\beta}{2}\right) \right)^{m-1} R_1 \pi \quad (5.9)$$

for all $m \geq 1$. Note that the specialization $\beta = \pi/2$ in the above formula transforms it, as expected, into Eq. (5.4).

5.2. Infinite levels and infinite lengths

In this subsection we apply infinity computing, and in particular the grossone-based system as announced before, to levels and lengths of the previous examples employing arc constructions. The first important difference is between the limit figure or set, if it exists, in the conventional sense of topological convergence and the figure at an infinite level m allowed in the grossone-based system (see, e.g. [14] and its references). In other words, there are no limits either of numerical sequences, or of functions, or, as in our case, of sequences of subsets of the plane like $\{L_m\}_{m \in \mathbb{N}}$, in the new system.

Using the classic setting, the only thing that can be said is that

$$\begin{aligned} \lim_{m \rightarrow \infty} l(L_m) &= \lim_{m \rightarrow \infty} l(G_m) = \lim_{m \rightarrow \infty} l(K_m) = \\ &= \lim_{m \rightarrow \infty} l(C_m) = \lim_{m \rightarrow \infty} l(P_{\beta, m}) = \lim_{m \rightarrow \infty} l(P_{\beta', m}) = +\infty \end{aligned} \quad (5.10)$$

for all fixed $\beta, \beta' \in]0, \pi[$. In the new setting, considering for example the infinite level $m = \mathbb{1}$, from (5.4), (5.5), (5.6), (5.7) and (5.9) we get

$$\begin{aligned} l(L_{\mathbb{1}}) &= \left(\sqrt{2}\right)^{\mathbb{1}-1} R_1 \pi, & l(G_{\mathbb{1}}) &= \left(\frac{3}{2}\right)^{\mathbb{1}-1} R_1 \pi, \\ l(K_{\mathbb{1}}) &= \frac{2^{\mathbb{1}}}{3^{(\mathbb{1}+1)/2}} R_1 \pi, & & \\ l(C_{\mathbb{1}}) &= \frac{17 \cdot 2^{\mathbb{1}-2}}{9} \left(\frac{\sin(19\pi/72)}{\cos(\pi/36)}\right)^{\mathbb{1}-1} R_1 \pi \end{aligned} \quad (5.11)$$

and

$$l(P_{\beta, \mathbb{1}}) = \left(\sin\left(\frac{\beta}{2}\right) + \cos\left(\frac{\beta}{2}\right)\right)^{\mathbb{1}-1} R_1 \pi$$

for all fixed $\beta \in]0, \pi[$. It is then remarkable that we no longer have infinities all equal and indistinguishable as in (5.10), but for example we can deduce that

$$\begin{aligned} \mathbb{1} < l(K_{\mathbb{1}}) < l(L_{\mathbb{1}}) < l(C_{\mathbb{1}}) < l(G_{\mathbb{1}}), \\ l(P_{\beta, \mathbb{1}}) < l(K_{\mathbb{1}}) &\Leftrightarrow \sin \beta < \frac{1}{3} \\ &\Leftrightarrow \beta \in \left]0, \arcsin\left(\frac{1}{3}\right) \left[\cup \right] \pi - \arcsin\left(\frac{1}{3}\right), \pi \left[\right. \end{aligned} \quad (5.12)$$

or

$$\mathbb{1} < l(P_{\beta, \mathbb{1}}) < l(P_{\beta', \mathbb{1}}) < l(L_{\mathbb{1}}) < l(C_{\mathbb{1}}) < l(G_{\mathbb{1}})$$

for all $\beta, \beta' \in]0, \pi[$ such that $|\beta - \pi/2| > |\beta' - \pi/2| > 0$, and many other similar relations (see below and the discussions in [3, 10, 49, 48, 50] with the references therein). For instance we can easily compare the length (or rather lengths, because actually there are infinitely many of them) obtained in [49] for the von Koch curve and our length $l(K_{\mathbb{1}})$. In [49] a symbol like $P_{\mathbb{1}}$ denotes the perimeter of the *von Koch snowflake* after $\mathbb{1}$ steps in its construction starting from an equilateral triangle of side ℓ at the zero step. We

have $P_{\textcircled{1}} = \ell \cdot 4^{\textcircled{1}}/3^{\textcircled{1}-1}$ (see [49, page 26]). To make an interesting comparison between our construction through an arc-based system and a more classical construction used in [49], we can set $2R_1 = \ell$, so

$$\frac{P_{\textcircled{1}}}{3} \cdot \frac{2R_1}{\ell} = \left(\frac{4}{3}\right)^{\textcircled{1}} \cdot 2R_1 \quad (5.13)$$

represents the length of the von Koch curve (after $\textcircled{1}$ steps) using the classical construction starting from a segment of length $2R_1$. This means that (5.13) is the right value which makes a lot of sense to compare with our $l(K_{\textcircled{1}})$. Denoting the value in (5.13) by $l(K_{\textcircled{1}}^*)$, we have

$$\frac{l(K_{\textcircled{1}})}{l(K_{\textcircled{1}}^*)} = \frac{(2^{\textcircled{1}}/3^{(\textcircled{1}+1)}/2) \cdot R_1 \pi}{(4/3)^{\textcircled{1}} \cdot 2R_1} = \frac{\pi}{4} \cdot \left(\frac{\sqrt{3}}{2}\right)^{\textcircled{1}-1}$$

which is an infinitesimal number. Therefore this means that the length $l(K_{\textcircled{1}})$ obtained by our arc-based construction, despite being infinite, it is infinitely smaller than $l(K_{\textcircled{1}}^*)$.

As another example, also note that reversing the relation “ $<$ ” in (5.12) between $l(P_{\beta, \textcircled{1}})$ and $l(K_{\textcircled{1}})$ we get

$$\begin{aligned} l(P_{\beta, \textcircled{1}}) > l(K_{\textcircled{1}}) &\Leftrightarrow \sin \beta \geq \frac{1}{3} \\ &\Leftrightarrow \beta \in \left[\arcsin\left(\frac{1}{3}\right), \pi - \arcsin\left(\frac{1}{3}\right) \right]. \end{aligned} \quad (5.14)$$

The reader who is not very familiar with infinity computing will perhaps be surprised by the appearance of “ \geq ” in (5.14), but he can easily verify this by doing a bit of calculations.

Another important difference with respect to classical analysis is that we can compute the results for a number of infinite levels, for example $m = \textcircled{1}/2$, $2\textcircled{1}/3 + 5$, $\textcircled{1} - 1$, etc. It is also possible to consider values greater than $\textcircled{1}$ by using many chained sequences (for more details on the basic principles of the new system see [48, 50]).

Let us assume, by way of example, that we wanted to compare $l(L_m)$ for $m = \textcircled{1}/2 + 1$ and $l(P_{\beta, m})$ for $m = \textcircled{1}$ (and $\beta \in]0, \pi[$ as above), i.e. the two infinite lengths $l(L_{\textcircled{1}/2+1})$ and $l(P_{\beta, \textcircled{1}})$. From (5.4) and (5.9) we get

$$\begin{aligned} (\sqrt{2})^{\textcircled{1}/2} &> \left(\sin\left(\frac{\beta}{2}\right) + \cos\left(\frac{\beta}{2}\right) \right)^{\textcircled{1}-1} \\ \Leftrightarrow (\sqrt[4]{2})^{\textcircled{1}} &> \left(\sin\left(\frac{\beta}{2}\right) + \cos\left(\frac{\beta}{2}\right) \right)^{\textcircled{1}} \cdot \frac{1}{\sin\left(\frac{\beta}{2}\right) + \cos\left(\frac{\beta}{2}\right)} \quad (5.15) \\ \Leftrightarrow \sqrt[4]{2} &\geq \sin\left(\frac{\beta}{2}\right) + \cos\left(\frac{\beta}{2}\right) \end{aligned}$$

(note the appearance of “ \geq ” in the third line of (5.15)). Since $\beta \in]0, \pi[$, we conclude that

$$\begin{aligned} l(L_{\textcircled{1}/2+1}) &> l(P_{\beta, \textcircled{1}}) \\ \iff \frac{\pi}{2} > \left| \beta - \frac{\pi}{2} \right| &\geq \frac{\pi}{2} - 2 \arcsin \left(\frac{\sqrt[4]{2} - \sqrt{2} - \sqrt{2}}{2} \right) \approx 1.14371774 \\ \iff \beta &\in]0, \approx 0.427078587] \cup [\approx 2.71451407, \pi]. \end{aligned}$$

Employing infinity computing, similar computations can be performed over real coastlines, whenever their geometric shapes are sufficiently clear defined (see Sect. 4).

We close this section with some considerations that we believe will be useful to the reader on the current lines of research that concern not infinite numbers properly saying, but “infinitely large” ones. In reality, these are finite ordinary numbers, but so large that they cannot be written using common notations (for example, $602.2 \times 10^{21} = 6.022 \times 10^{23}$ represent Avogadro’s number in engineering and scientific notation, respectively). Numbers equal or larger than 1 *googol*, i.e. 10^{100} ,³ are called unimaginable numbers. The most used notations to represent unimaginable numbers, usually enormously larger than 1 googol, are *Knuth up-arrow notation*, *Conway chained arrow notation*, *Steinhaus–Moser notation*,⁴ and others. For precise definitions and some properties see [13, 33] and the references therein. The unimaginable numbers such as *megiston*, *mega*, *Moser’s number*, *Graham’s number*, etc. (see [13, 33]), from a computational point of view they are in fact infinite numbers. This is in fact the only practical way to be able to carry out explicit calculations with them. They can therefore be employed at a symbolic level of computation as we have done in this section with grossone, and generally no more than one at a time because no precise relationships are known between them other than some enormously, “unimaginably coarse” bounds. Even the symbols used for mega and megiston are very suggestive because they resemble the one for the grossone. The mega is in fact usually denoted by $\textcircled{2}$ and the megiston by $\textcircled{10}$.

6. Conclusions

In the first part of this paper we considered recursive systems based on arcs of circumference (see (2.1) and (2.14)). Then we considered in Sect. 3 generalizations to other types of curves and we have highlighted what we have called the “universal property” of the arc system. In particular, we have given

³1 googol is close to 70! and, more significantly from a physical point of view, is it rather larger than the *Eddington number* N_{Edd} which represents the number of protons in the observable universe and is estimated to be around 10^{80} . Thus, numbers larger than 1 googol increasingly lose all physical meaning. Even the company Google Inc. owes its name to googol.

⁴Interestingly, Steinhaus refers to the same author as [51], albeit in a completely different context.

examples built on arcs of the golden spiral, a curve of primary importance in nature. We then devoted Sect. 4 to an initial discussion on the implications for coastlines and above all for HBBs, from which part of the entire paper draws inspiration. Sect. 5 builds a three-pillar bridge between the previously described recursive systems, coastlines and infinity computing.

Much future work can be done starting from this paper and many implications are already under discussion within the research group of which the authors are part. Here we outline three main directions. The first leads to applications to coastal profiles. We find it very interesting to try to use the tools of Sect. 2 and above all Sect. 3 to describe real cases of HBBs. A second direction lies in the union between infinity computing and recursive systems, in particular those based on curves other than arcs of circumference. A third direction proceeds towards pure mathematics, geometry and fractals (recall, e.g. [44]). Many new geometric structures and new properties can also be discovered with such recursive systems.

Acknowledgment

This work was carried out under the auspices of the GNFM of the *Istituto Nazionale di Alta Matematica “F. Severi”* (INDAM).

The authors would also like to thank the anonymous reviewers for their careful reading of the manuscript and their comments.

References

- [1] Abdul-Kareem, R., Asare, N., Angnuureng, D., Brempong, E.K.: Shoreline variability of a bay beach: The case of Apam Beach, Ghana. *Estuaries and Coasts* **45**, 2373–2386 (2022). DOI 10.1007/s12237-022-01110-9
- [2] Anatriello, G., Vincenzi, G.: Logarithmic spirals and continue triangles. *Journal of Computational and Applied Mathematics* **296**, 127–137 (2016). DOI 10.1016/j.cam.2015.09.004
- [3] Antoniotti, L., Caldarella, F., Maiolo, M.: Infinite numerical computing applied to Hilbert’s, Peano’s, and Moore’s curves. *Mediterranean Journal of Mathematics* **17**, 99 (2020). DOI 10.1007/s00009-020-01531-5
- [4] Avdeev, A.V., Goriounov, E.V., Lavrentiev, M.M., Spigler, R.: A behavior-oriented model for long-term coastal profile evolution: Validation, identification, and prediction. *Applied Mathematical Modelling* **33**, 3981–3996 (2009). DOI 10.1016/j.apm.2009.01.010
- [5] Baramiya, D., Lavrentiev, M., Spigler, R.: Predicting coastal profiles evolution from a diffusion model based on real data. *Applied Mathematical Modelling* **111**, 713–726 (2022). DOI 10.1016/j.apm.2022.06.041
- [6] De la Beche, H.T.: *Geological Manual*. C. Knight, London (1833). 3d ed., considerably enl.
- [7] Benedet, L., da Fontoura Klein, A.H., Hsu, J.R.: Practical insights and applicability of empirical bay shape equations. *Coastal Engineering* **2004**, 2181–2193 (2005). DOI 10.1142/9789812701916_0175

- [8] Bremner, J.M.: Properties of logarithmic spiral beaches with particular reference to Algoa Bay. In: A. McLachlan, T. Erasmus (eds.) *Sandy Beaches as Ecosystems, Developments in Hydrobiology*, vol. 19, pp. 97–113. Springer, Dordrecht (1983). DOI 10.1007/978-94-017-2938-3_6
- [9] Caldarola, F.: The exact measures of the Sierpiński d -dimensional tetrahedron in connection with a Diophantine nonlinear system. *Communications in Nonlinear Science and Numerical Simulation* **63**, 228–238 (2018). DOI 10.1016/j.cnsns.2018.02.026
- [10] Caldarola, F.: The Sierpiński curve viewed by numerical computations with infinities and infinitesimals. *Applied Mathematics and Computation* **318**, 321–328 (2018). DOI 10.1016/j.amc.2017.06.024
- [11] Caldarola, F., d’Atri, G., Maiolo, M., Pirillo, G.: New algebraic and geometric constructs arising from Fibonacci numbers. In honor of Masami Ito. *Soft Computing* **24(23)**, 17497–17508 (2020). DOI 10.1007/s00500-020-05256-1
- [12] Caldarola, F., d’Atri, G., Maiolo, M., Pirillo, G.: The sequence of Carboncettus octagons. In: Y.D. Sergeyev, D. Kvasov (eds.) *Proc. of the 3rd Intern. Conf. “Numerical Computations: Theory and Algorithms”*, *LNCS*, vol. 11973, pp. 373–380. Springer, Cham (2020). DOI 10.1007/978-3-030-39081-5_32
- [13] Caldarola, F., d’Atri, G., Mercuri, P., Talamanca, V.: On the arithmetic of Knuth’s powers and some computational results about their density. In: Y.D. Sergeyev, D. Kvasov (eds.) *Proc. of the 3rd Intern. Conf. “Numerical Computations: Theory and Algorithms”*, *LNCS*, vol. 11973, pp. 381–388. Springer, Cham (2020). DOI 10.1007/978-3-030-39081-5_33
- [14] Caldarola, F., Maiolo, M.: On the topological convergence of multi-rule sequences of sets and fractal patterns. *Soft Computing* **24**, 17737–17749 (2020). DOI 10.1007/s00500-020-05358-w
- [15] Caldarola, F., Maiolo, M., Solferino, V.: A new approach to the Z -transform through infinite computation. *Communications in Nonlinear Science and Numerical Simulation* **82**, 105019 (2020). DOI 10.1016/j.cnsns.2019.105019
- [16] da Fontoura Klein, A.H., Vargas, A., Raabe, A.L.A., Hsu, J.R.: Visual assessment of bayed beach stability with computer software. *Computers & Geosciences* **29(10)**, 1249–1257 (2003). DOI 10.1016/j.cageo.2003.08.002
- [17] Davidson, M.: Forecasting coastal evolution on time-scales of days to decades. *Coastal Engineering* **168**, 103928 (2021). DOI 10.1016/j.coastaleng.2021.103928
- [18] Falcone, A., Garro, A., Mukhametzhanov, M.S., Sergeyev, Y.D.: A Simulink-based software solution using the Infinity Computer methodology for higher order differentiation. *Applied Mathematics and Computation* **409**, 125606 (2021). DOI 10.1016/j.amc.2020.125606
- [19] Falconer, K.: *Fractal Geometry. Mathematical Foundations and Applications*, third edn. John Wiley & Sons, Chichester (UK) (2014)
- [20] Gargano, F., Ponetti, G., Sammartino, M., Sciacca, V.: Complex singularities in KdV solutions. *Ricerche di Matematica* **65**, 479–490 (2016). DOI 10.1007/s11587-016-0269-9
- [21] Hsu, J.R.C., Evans, C.: Parabolic bay shapes and applications. *Proceedings of the Institution of Civil Engineers* **87**, 557–570 (1989)
- [22] Hsu, J.R.C., Lee, J.L., Klein, A.H.F., González, M., Medina, R.: Headland-Bay Beaches: Static Equilibrium Concept for Shoreline Management, *Advanced*

Series on Ocean Engineering, vol. 53. World Scientific, Singapore (2021). DOI 10.1142/12026

- [23] Huynh, H.N., Chew, L.Y.: Arc-fractal and the dynamics of coastal morphology. *Fractals* **19**, 141–162 (2011). DOI 10.1142/S0218348X11005178
- [24] Kaergaard, K., Fredsoe, J.: A numerical shoreline model for shorelines with large curvature. *Coastal Engineering* **74**, 19–32 (2013). DOI 10.1016/j.coastaleng.2012.11.011
- [25] Karunarathna, H., Horrillo-Caraballo, J.M., Reeve, D.E.: Prediction of cross-shore beach profile evolution using a diffusion type model. *Continental Shelf Research* **48**, 157–166 (2012). DOI 10.1016/j.csr.2012.08.004
- [26] Kimberley, M.M.: Fitting a logarithmic spiral to the shoreline of a headland-bay beach. *Computers & Geoscience* **15**, 1089–1108 (1989)
- [27] https://en.m.wikipedia.org/wiki/Koch_snowflake (). Last accessed: December 29, 2023
- [28] Larson, M., Le Xuan, H., Hanson, H.: Direct formula to compute wave height and angle at incipient breaking. *Journal of Waterway, Port, Coastal and Ocean Engineering* **136**, 119–122 (2010). DOI 10.1061/(ASCE)WW.1943-5460.000003
- [29] Lausman, R., Klein, A.H.F., Stive, M.J.F.: Uncertainty in the application of the parabolic bay shape equation: Part 1. *Coastal Engineering* **57**, 132–141 (2010). DOI 10.1016/j.coastaleng.2009.09.009
- [30] Lausman, R., Klein, A.H.F., Stive, M.J.F.: Uncertainty in the application of the parabolic bay shape equation: Part 1. *Coastal Engineering* **57**, 142–151 (2010). DOI 10.1016/j.coastaleng.2009.10.001
- [31] Layeghi, R.: Application of parabolic bay shaped beach model concept to natural beaches in Northern Cyprus. Master's thesis, Eastern Mediterranean University, Faculty of Engineering, Dept. of Civil Engineering (2014)
- [32] LeBlond, P.H.: An explanation of the logarithmic spiral plan shape of headlandbay beaches. *Journal of Sediment Petrology* **49**, 1093–1100 (1979)
- [33] Leonardis, A., d'Atri, G., Caldarella, F.: Beyond Knuth's notation for unimaginable numbers within computational number theory. *International Electronic Journal of Algebra* **31**, 55–73 (2022). DOI 10.24330/ieja.1058413
- [34] Li, B., Zhuang, Z., Cao, L., Du, F.: Application of the static headland-bay beach concept to a sandy beach: A new elliptical model. *Journal of Ocean University of China* **19**, 81–89 (2020). DOI 10.1007/s11802-020-3899-1
- [35] Lim, C., Hwang, S., Lee, J.L.: An analytical model for beach erosion downdrift of groins: case study of Jeongdongjin Beach, Korea. *Earth Surface Dynamics* **10**, 151–163 (2022). DOI 10.5194/esurf-10-151-2022
- [36] Manakul, C., Mohanasundaram, S., Weesakul, S., Shrestha, S., Ninsawat, S., Chonwattana, S.: Classifying headland-bay beaches and dynamic coastal stabilization. *Journal of Marine Science and Engineering* **10**, 1363 (2022). DOI 10.3390/jmse10101363
- [37] Mandelbrot, B.: How long is the coast of Britain? Statistical self-similarity and fractional dimension. *Science* **156**, 636–638 (1967). DOI 10.1126/science.156.3775.636
- [38] Mandelbrot, B.B.: *The Fractal Geometry of Nature*. W. H. Freeman and Co., New York (1982)

- [39] Moreno, L.J., Kraus, N.C.: Equilibrium shape of headland-bay beaches for engineering design. In: *Proceedings of the Coastal Sediments 1999*, vol. 1, pp. 860–875. American Society of Civil Engineers, New York (1999)
- [40] Panchang, V.G., Pearce, B.R., Wei, G., Cushman-Roisin, B.: Solution of the mild-slope wave problem by iteration. *Applied Ocean Research* **13**, 187–199 (1991). DOI 10.1016/S0141-1187(05)80074-4
- [41] Robinet, A., Idier, D., Castelle, B., Marieu, V.: A reduced-complexity shoreline change model combining longshore and cross-shore processes: the LX-Shore model. *Environmental Modelling & Software* **109**, 1–16 (2018). DOI 10.1016/j.envsoft.2018.08.010
- [42] Robinson, A.: *Non-standard Analysis*. Princeton University Press (1966)
- [43] Roelvink, D., Huisman, B., Elghandour, A., Ghonim, M., Reyns, J.: Efficient modeling of complex sandy coastal evolution at monthly to century time scales. *Frontiers in Marine Science* **7** (2020). DOI 10.3389/fmars.2020.00535
- [44] Ryde, K.: Iterations of the Lévy C curve. <http://user42.tuxfamily.org/c-curve/index.html> (2022)
- [45] Sergeev, Y.D.: Blinking fractals and their quantitative analysis using infinite and infinitesimal numbers. *Chaos, Solitons & Fractals* **33**(1), 50–75 (2007)
- [46] Sergeev, Y.D.: Measuring fractals by infinite and infinitesimal numbers. *Mathematical Methods, Physical Methods & Simulation Science and Technology* **1**, 217–237 (2008)
- [47] Sergeev, Y.D.: Evaluating the exact infinitesimal values of area of Sierpinski’s carpet and volume of Menger’s sponge. *Chaos, Solitons & Fractals* **42**, 3042–3046 (2009)
- [48] Sergeev, Y.D.: Lagrange Lecture: Methodology of numerical computations with infinities and infinitesimals. *Rendiconti del Seminario Matematico dell’Università e del Politecnico di Torino* **68**, 95–113 (2010)
- [49] Sergeev, Y.D.: The exact (up to infinitesimals) infinite perimeter of the Koch snowflake and its finite area. *Communications in Nonlinear Science and Numerical Simulation* **31**, 21–29 (2016)
- [50] Sergeev, Y.D.: Numerical infinities and infinitesimals: Methodology, applications, and repercussions on two Hilbert problems. *EMS Surveys in Mathematical Sciences* **4**, 219–320 (2017)
- [51] Steinhaus, H.: Length, shape and area. *Colloquium Mathematicum* **3**, 1–13 (1954). DOI 10.4064/cm-3-1-1-13
- [52] Terpstra, P.D., Chrzastowski, M.J.: Geometric trends in the evolution of a small log-spiral embayment on the Illinois shore of Lake Michigan.”. *Journal of Coastal Research* **8**, 603–617 (1992)
- [53] Vorobiev, N.N.: *Fibonacci Numbers*. Birkhäuser, Basel (2002)
- [54] de Vriend, H.J., Capobianco, M., Chesher, T., de Swart, H.E., Latteux, B., Stive, M.J.F.: Approaches to long-term modelling of coastal morphology: A review. *Coastal Engineering* **21**, 225–269 (1993). DOI 10.1016/0378-3839(93)90051-9
- [55] Yasso, W.E.: Plan geometry of headland-bay beaches. *The Journal of Geology* **73**, 702–714 (1965)

- [56] Zayed, E.M.E., Rahman, H.M.A.: On using the modified variational iteration method for solving the nonlinear coupled equations in the mathematical physics. *Ricerche di matematica* **59**, 137–159 (2010). DOI 10.1007/s11587-010-0075-8

Fabio Caldarola
Department of Environmental Engineering,
Cubo 42/B, Ponte Bucci,
University of Calabria,
87036 Rende (CS), Italy
e-mail: fabio.caldarola@unical.it

Manuela Carini
Department of Environmental Engineering,
Cubo 42/B, Ponte Bucci,
University of Calabria,
87036 Rende (CS), Italy
e-mail: manuela.carini@unical.it

Mario Maiolo
Department of Environmental Engineering,
Cubo 42/B, Ponte Bucci,
University of Calabria,
87036 Rende (CS), Italy
e-mail: mario.maiolo@unical.it

Maria Anastasia Papaleo
e-mail: maria.anastasiapapaleo@gmail.com